Nonlinear Observer for Tightly Coupled Integration of Pseudorange and Inertial Measurements

Tor A. Johansen and Thor I. Fossen

***Abstract*— A global nonlinear algebraic transform of nonlinear pseudorange measurement equations enables navigation solutions based on a globally valid linear time-varying measurement model. Using an interconnection of a nonlinear attitude observer and a translational motion observer based on pseudorange and range–range measurements, a tightly coupled integrated aided inertial navigation system is designed. The attitude observer uses a proper acceleration estimate from the translational motion observer as a reference vector for the accelerometer measurement. This leads to a feedback interconnection that is shown to be globally exponentially stable under some conditions on the tuning parameters. The model transformation has eliminated the information about a certain nonlinear relationship that exists among the measurements. While this enables the global solution to be found, it also leads to loss of estimation accuracy when there is measurement noise. In order to recover close-to-optimal (minimum variance) estimates, the observer estimates are only used to generate a locally linearized time-varying model that is subsequently employed by a Kalman filter, without loss of global convergence.**

***Index Terms*— Inertial navigation, Kalman filter, nonlinear observers, pseudorange measurements.**

I. Introduction

RANGE measurement systems for vehicle navigation typically involve a receiver on the vehicle that receives signals from transponders[1] at known locations. The receiver measures signal time of arrival, phase difference, or some other variable that is proportional to the range. The geometric range is a nonlinear function of vehicle and transponder positions given by their Euclidean distance. Since the geometric range is not measured directly, one usually employs a pseudorange measurement model with a bias parameter due to effects such as clock synchronization errors.

Usually at least four measurements are needed to estimate the four variables: three position coordinates and a bias parameter. With a sufficient number of pseudorange measurements, the global nonlinear algebraic equations of the position estimation problem have two solutions, except in cases with at least five measurements, where the solution is typically unique [1]–[3]. Although the global algebraic solution can be used directly, an observer employs dynamic models and other measurements to improve the accuracy and robustness.

Inertial sensors such as accelerometers and rate gyros can be used to estimate position and velocity by integrating the kinematic equations. Since sensor biases and other errors are accumulated in this process, leading to unbounded errors on the position estimates, inertial navigation systems can be aided by range measurements that can be used to stabilize these errors using a state estimator. There are two main design philosophies for such state estimators: 1) loosely and 2) tightly coupled integration [4], [5]. In a loosely integrated scheme, a standalone estimate of position and velocity in an earth-fixed Cartesian coordinate frame is first found using only the pseudorange measurements. These position and velocity estimates are then used as measurements in a state observer that integrates them with the inertial measurements. In a tightly integrated scheme, the pseudorange measurements are directly used in a state observer together with the inertial measurements. While the advantage of loosely coupled integration is a high degree of modularity, the advantage of tightly coupled integration is increased accuracy and fault tolerance.

Typical approaches to design of estimators for tightly integrated inertial navigation based on pseudorange measurements use a local linearization approach as the basis for a nonlinear Kalman filter or particle filter [4]–[6]. This is a state-of-the-art solution that has been extremely successful and reaps the benefits of the optimality of the Kalman filter in the presence noise. However, it does not come without drawbacks such as stability conditions that are hard to verify *a priori*, possibly limited region of convergence, and relatively high computational complexity. Johansen and Fossen [7] presented a nonlinear observer approach to tightly integrated inertial navigation. The method proves exponential stability with a semiglobal region of attraction with respect to attitude estimate initialization, but only local region of attraction with respect to position and velocity estimate initialization errors. In [8]–[10], the design of tightly integrated nonlinear observers for attitude, position, and velocity using hydroacoustic range measurements is investigated. Using mathematical manipulations such as time-differentiation, algebraic manipulation, and introduction of new variables, they reformulate the vehicle's kinematic model into a linear time-varying (LTV) model which is

Manuscript received November 28, 2015; revised January 24, 2016; accepted January 29, 2016. Date of publication February 24, 2016; date of current version October 14, 2016. Manuscript received in final form January 30, 2016. This work was supported by the Research Council of Norway, Statoil, Det Norske Veritas & Germanischer Lloyd, and Sintef through the Centers of Excellence Funding Scheme under Grant 223254 and in part by the Centre for Autonomous Marine Operations and Systems under Grant 221666. Recommended by Associate Editor N. van de Wouw. *(Corresponding author: Tor A. Johansen.)*

The authors are with the Center for Autonomous Marine Operations and Systems, Department of Engineering Cybernetics, Norwegian University of Science and Technology, Trondheim 7491, Norway (e-mail: tor.arne.johansen@itk.ntnu.no; thor.fossen@ntnu.no).

Color versions of one or more of the figures in this paper are available online at http://ieeexplore.ieee.org.

Digital Object Identifier 10.1109/TCST.2016.2524564

[1]Note that we use the term transponder in a generalized way, meaning anything from an acoustic transponder, to a navigation satellite in space, radio beacons, or laser ranging system reflector.

equivalent to the nonlinear model in the noise-free case. Hence, one can apply the standard Kalman filter to achieve uniform global asymptotic stability.

In this brief, we describe a tightly integrated inertial navigation observer using an attitude estimate from a globally exponentially stable (GES) attitude observer [11] (see also [12], [13] for similar attitude observers) in combination with a translational motion observer based on a quasi-linear LTV model using pseudorange measurements. In order to achieve high performance with vehicles that may have significant persistent accelerations, the attitude observer uses accelerometer and magnetometer vector measurements, where the proper acceleration reference vector accounts for vehicle motion in addition to gravity using feedback from the vehicle acceleration estimate of the translational motion observer. This leads to a nonlinear feedback interconnection between the two nonlinear observers that needs to be considered in the design and analysis, similar to [11]. Johansen *et al.* [14] describe the use of the quasi-linear model approach to position estimation-based pseudorange measurements, but with a stochastic vehicle model that does not assume inertial or attitude sensors. This brief extends these results by considering tightly coupled integration with inertial measurements that can achieve significantly better performance. This extension is nontrivial since we consider accelerated vehicles that require a feedback from an acceleration estimate, and the pseudorange measurement model is LTV, meaning that the fixed-gain strategy and analysis in [11] must be extended to time-varying gain and LTV analysis.

In contrast to [8]–[10], we avoid augmentation of the model by fully exploiting the structure of the transformed measurement equation for the benefit of simple tuning and low computational complexity in combination with GES. Moreover, minimum variance estimation accuracy issues that arise with measurement noise in combination with information loss caused by algebraic elimination of nonlinearities can be addressed via a final-stage GES Kalman–Bucy filter similar to [14].

A. Notation

We may use a superscript index to indicate the coordinate system in which a given vector is decomposed, and thus, x^a and x^b refers to the same vector decomposed in the coordinated systems indexed by a and b, respectively. The rotation from coordinate frame a to b represented by a matrix is denoted by $R_a^b \in \mathbb{R}^{3\times 3}$. For a vector $x \in \mathbb{R}^3$, let $\|x\|_2$ denote the Euclidean norm and define the skew-symmetric matrix

$$S(x) := \begin{pmatrix} 0 & -x_3 & x_2 \\ x_3 & 0 & -x_1 \\ -x_2 & x_1 & 0 \end{pmatrix}.$$

The skew-symmetric part of a matrix A is denoted by $\mathbb{P}_a(A) = (1/2)(A - A^T)$. The linear function $\mathrm{vex}(A)$ such that $\mathrm{vex}(S(x)) = x$ is well defined for all 3×3 skew-symmetric matrix arguments. The rate of rotation of the coordinate system indexed by b with respect to a, decomposed in c, is denoted ω_{ab}^c. We use b for the vehicle body-fixed coordinate system, n for the north–east–down (NED) local tangential system, and i for the earth-centered inertial (ECI) coordinate system. For a matrix A, let A^+ denote the left Moore–Penrose pseudoinverse and $\underline{\sigma}(A)$ its smallest singular value.

II. Models and Preliminaries

A. Vehicle Kinematics

The vehicle kinematic model is given by (see [4])

$$\dot{p}^n = v^n \tag{1}$$
$$\dot{v}^n = R_b^n f^b + g^n \tag{2}$$
$$\dot{R}_b^n = R_b^n S\left(\omega_{ib}^b\right) \tag{3}$$

where p^n, v^n, and f^n are position, velocity, and proper acceleration in NED, respectively. The attitude of the vehicle is described by a rotation matrix R_b^n representing the rotation from body to NED; ω_{ib}^b represents the rotation rate of body with respect to ECI and g^n denotes the gravity vector. For simplicity of presentation, we assume NED to be an inertial frame, i.e., neglect the rotation of the earth, and will remark later on how the results can be extended to avoid the errors made by this assumption.

B. Inertial Sensor Models

The inertial sensor model is based on the strapdown assumption, i.e., the inertial measurement unit (IMU) is fixed to the body frame

$$f_{\mathrm{IMU}}^b = f^b + \epsilon_f \tag{4}$$
$$\omega_{ib,\mathrm{IMU}}^b = \omega_{ib}^b + b + \epsilon_\omega \tag{5}$$
$$\dot{b} = \epsilon_b \tag{6}$$

where ϵ_f and ϵ_ω account for noise, and b denotes the rate gyro bias that is driven by the noise ϵ_b and assumed to satisfy $\|b\|_2 \leq M_b$ for some known bound M_b. We assume that accelerometer drift and biases are compensated for using a bias estimation method such as [15], which can be included in cascade with the proposed estimator. The magnetometer measurement gives the 3-D earth magnetic vector field decomposed in the body frame $m_{\mathrm{mag}}^b = m^b + \epsilon_m$, where ϵ_m is noise.

C. Pseudorange Measurement Model

Range is often measured indirectly by some receiver that measures signal time of arrival, phase difference, or some other variable that is proportional to the range (see [3]). The geometric range

$$\varrho_i = \left\| p^n - p_i^n \right\|_2 \tag{7}$$

is a nonlinear function of the vehicle position p^n and the ith transponder position p_i^n, given by their Euclidean distance. Since the geometric range is not measured directly, one usually needs a pseudorange measurement model that includes an additional bias parameter $\beta \in \mathbb{R}$ due to unknown clock synchronization errors (i.e., $\beta := c\Delta_c$, where Δ_c is the receiver clock bias and c is the wave speed) or other unknown effects. The pseudorange measurement model is

$$y_i = \varrho_i + \beta + \epsilon_{yi} \tag{8}$$

for $i = 1, 2, \ldots, m$, where y_i is a pseudorange measurement, ϵ_{yi} is noise, and m is the number of measurements.

Despite the nonlinear nature of the pseudorange measurement model, we can exploit its quadratic character to get a relatively simple quasi-linear form using a standard nonlinear transformation [1]–[3]. In order to present this model, let a known fixed reference position p_0^n be chosen, and define the transponder line-of-sight vectors $\breve{p}_i^n := p_i^n - p_0^n$ relative to this reference position for every i. We define $p_\Delta^n = p^n - p_0^n$ and get from (7) and (8)

$$(y_i - \epsilon_{yi} - \beta)^2 = \left(p_\Delta^n - \breve{p}_i^n\right)^T \left(p_\Delta^n - \breve{p}_i^n\right). \tag{9}$$

Expanding and rearranging terms gives

$$2\left(-\left(\breve{p}_i^n\right)^T, y_i - \epsilon_{yi}\right)x = r + (y_i - \epsilon_{yi})^2 - \|\breve{p}_i\|_2^2 \tag{10}$$

where $x := (p_\Delta^n; \beta)$, and we have introduced an auxiliary variable $r := \beta^2 - \|p_\Delta^n\|_2^2 = -x^T M x$ with $M := \mathrm{diag}(1, 1, 1, -1)$. Stacking instances of (10) for $i = 1, 2, \ldots, m$ into matrices and vectors gives the quasi-linear relationship

$$2C_{zw}x = r\ell + z + \eta \tag{11}$$

where the matrix $C_{zw} \in \mathbb{R}^{m\times 4}$ is

$$C_{zw} := \begin{pmatrix} -\left(\breve{p}_1^n\right)^T & y_1 \\ \vdots & \\ -\left(\breve{p}_m^n\right)^T & y_m \end{pmatrix}$$

$\ell \in \mathbb{R}^m$ is given by $\ell_i := 1$, $z \in \mathbb{R}^m$ has components $z_i := y_i^2 - \|\breve{p}_i^n\|_2^2$, and $\eta \in \mathbb{R}^m$ depends on the noise. Its elements are $\eta_i = \epsilon_{yi}^2 + 2(\beta - y_i)\epsilon_{yi}$.

It is convenient to eliminate r from (11) by defining $m - 1$ computed measurements using single differences of the squared range measurements $\delta_i = z_i - z_m$, for $i = 1, 2, \ldots, m-1$

$$2C_{\delta x}x = \delta + \varepsilon \tag{12}$$

where the matrix $C_{\delta x} \in \mathbb{R}^{(m-1)\times 4}$ is

$$C_{\delta x} := \begin{pmatrix} \left(p_m^n - p_1^n\right)^T & y_1 - y_m \\ \vdots & \\ \left(p_m^n - p_{m-1}^n\right)^T & y_{m-1} - y_m \end{pmatrix}$$

and $\varepsilon \in \mathbb{R}^{m-1}$ has elements $\varepsilon_i = \eta_i - \eta_m$.

Assumption 1: Transponder positions p_i^n are known.

Assumption 2: The range measurement bias is constant

$$\dot{\beta} = 0. \tag{13}$$

Algebraic solutions to (11) for the case $m \geq 4$ and (12) for the case $m \geq 5$ are described in the Appendix. They can be directly used for accurate initialization, monitoring of performance, loosely coupled integration strategies, and so on.

III. Observer Design

We use the attitude observer described in Section III-A and combine that with a tightly coupled translational motion observer described in Section III-B, where an INS is aided by pseudorange measurements using the quasi-linear measurement model of Section II-C. A block diagram illustrating this observer structure is shown in Fig. 1.

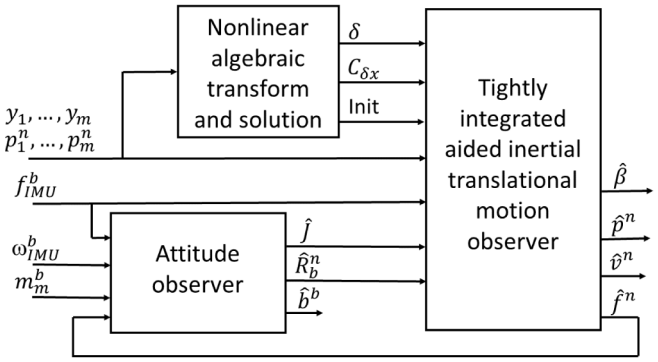

Fig. 1. Overall block diagram for tightly integrated observer.

A. Attitude Observer

We use the attitude observer from [11]

$$\dot{\hat{R}}_b^n = \hat{R}_b^n S\left(\omega_{ib,\mathrm{IMU}}^b - \hat{b}\right) + \sigma K_P J\left(t, \hat{R}_b^n\right)$$
$$\dot{\hat{b}} = \mathrm{Proj}\left(-k_I \mathrm{vex}\left(\mathbb{P}_a\left(\mathrm{sat}\left(\hat{R}_b^n\right)^T K_P J\left(t, \hat{R}_b^n\right)\right)\right), M_{\hat{b}}\right)$$

where $K_P > 0$ is a symmetric 3×3 gain matrix, $k_I > 0$ is a scalar gain, and $\sigma \geq 1$. The function $\mathrm{sat}(\cdot)$ is an element-wise saturation, while $\mathrm{Proj}(\cdot)$ is a parameter projection which ensures that $\|\hat{b}\|_2 \leq M_{\hat{b}}$, where $M_{\hat{b}} > M_b$ [11]. The parameter projection is assumed to have the functionality that if at any point in time the value $\hat{b}$ is outside the ball $\|\hat{b}\|_2 \leq M_{\hat{b}}$, its value is reset to the boundary of the ball: $\hat{b} \leftarrow M_{\hat{b}}\hat{b}/\|\hat{b}\|_2$. $J(\cdot) \in \mathbb{R}^{3\times 3}$ is a stabilizing injection term

$$J(t, \hat{R}_b^n) = \left(E^n - \hat{R}_b^n E^b\right)(E^b)^T$$

based on the vector measurements m_{mag}^b and f_{IMU}^b and their NED reference vectors m^n and $\hat{f}^n$ used to define vectors scaled by suitable nonzero terms

$$q_1^b = m_{\mathrm{mag}}^b/\|m_{\mathrm{mag}}^b\|_2, \quad q_2^b = f_{\mathrm{IMU}}^b/\|g^n\|_2$$
$$q_1^n = m^n/\|m^n\|_2, \quad q_2^n = \hat{f}^n/\|g^n\|_2$$

and the 3×3 matrices

$$E^b = \left(q_1^b,\ S(q_1^b)q_2^b,\ S^2(q_1^b)q_2^b\right)$$
$$E^n = \left(q_1^n,\ S(q_1^n)q_2^n,\ S^2(q_1^n)q_2^n\right).$$

The two reference vectors must not be parallel in order to guarantee observability of the attitude.

Assumption 3: There exists a constant $c_{\mathrm{obs}} > 0$ such that at all time $\|m^n \times \hat{f}^n\|_2 \geq c_{\mathrm{obs}}$.

Conditions for GES of this observer error dynamics are provided in [11] for the nominal case with $\hat{f}^n = f^n$.

Lemma 1: Assume that $\hat{f}^n = f^n$, there is no noise $\epsilon_f = \epsilon_m = 0$ and $\epsilon_b = 0$, and let $K_P > 0$ and $k_I > 0$ be arbitrary. Then there exists a $\sigma^* \geq 1$ such that for all $\sigma \geq \sigma^*$, the origin of the attitude estimation error dynamics $\tilde{R} = R_b^n - \hat{R}_b^n$ and $\tilde{b} = b - \hat{b}$ is GES.

Remark 1: The estimate $\hat{R}_b^n \in \mathbb{R}^{3\times 3}$ may not have the properties of a rotation matrix, even though it converges asymptotically to a rotation matrix on SO(3). Lemma 1 is valid despite this fact, and in Section III-B, we show that this also has no consequences for the use of $\hat{R}_b^n$ in an estimator for

linear position, velocity, and acceleration. Nevertheless, one may choose to project $\hat{R}_b^n$ onto SO(3) to compute an attitude estimate represented, e.g., as Euler angles (see [11]).

B. Translational Motion Observer

In this section, we consider the estimation of the vehicle's position, linear velocity, and linear acceleration. The kinematic model (1)–(3) provides the basic relationship, having acceleration as input where an attitude estimate is employed to approximately transform the accelerometer measurement vector from body to NED. In addition, aiding from the pseudorange measurements is provided by using the globally valid LTV measurement model (12). Consider

$$\dot{\hat{p}}_\Delta^n = \hat{v}^n + K_{pp}(\delta - \hat{\delta}) \tag{14}$$

$$\dot{\hat{\beta}} = K_{\beta p}(\delta - \hat{\delta}) \tag{15}$$

$$\dot{\hat{v}}^n = \hat{f}^n + g^n + K_{vp}(\delta - \hat{\delta}) \tag{16}$$

$$\dot{\hat{\xi}} = -\sigma K_P J\left(t, \hat{R}_b^n\right) f_b^{\mathrm{IMU}} + K_{\xi p}(\delta - \hat{\delta}) \tag{17}$$

$$\hat{f}^n = \hat{R}_b^n f_{\mathrm{IMU}}^b + \xi \tag{18}$$

with $\hat{\delta} = 2C_{\delta x}\hat{x}$ and the gain matrices K_* are in general time varying. The estimated state vector is $\hat{\chi} = (\hat{x}; \hat{v}^n; \hat{f}^n) \in \mathbb{R}^{10}$ with $\hat{x} = (\hat{p}_\Delta^n; \hat{\beta})$. Note that for the purpose of analysis, (14)–(18) can be transformed into an LTV error system

$$\dot{\tilde{\chi}} = (A - KC)\tilde{\chi} + Bu + B\epsilon_u + K\varepsilon \tag{19}$$

with input

$$u = \tilde{R}\dot{f}^b + \tilde{R}S\left(\omega_{ib}^b\right) f^b - \hat{R}_b^n S(\tilde{b}) f^b \tag{20}$$

and ϵ_u is driven by the IMU noise ϵ_f and ϵ_ω, and

$$A := \begin{pmatrix} 0 & 0 & I_3 & 0 \\ 0 & 0 & 0 & 0 \\ 0 & 0 & 0 & I_3 \\ 0 & 0 & 0 & 0 \end{pmatrix}, \quad B := \begin{pmatrix} 0 \\ 0 \\ 0 \\ I_3 \end{pmatrix}$$

$$K := \begin{pmatrix} K_{pp} \\ K_{\beta p} \\ K_{vp} \\ K_{\xi p} \end{pmatrix}, \quad C := (2C_{\delta x} \quad 0 \quad 0).$$

Before we proceed with the stability analysis and gain conditions of the interconnected system, we need to investigate conditions when the translational motion error dynamics are uniformly observable (UO).

Assumption 4: There are available $m \geq 5$ pseudorange measurements $y = (y_1; y_2; \ldots; y_m)$, and there exists a constant $\underline{\sigma}^* > 0$ such that at all time $\underline{\sigma}(C_{\delta x}^T C_{\delta x}) \geq \underline{\sigma}^*$.

Remark 2: From the definition of $C_{\delta x}$, it is clear that Assumption 4 depends on both the geometry of the transponder configuration and the trajectory of the vehicle. It can be inferred from $C_{\delta x}$ that the assumption requires that all transponders are not located in the same plane. For further insight and interpretation, the reader is referred to [2].

Lemma 2: The LTV system (A, C) is UO.

Proof: Let $C_{\delta x}^{1:3} \in \mathbb{R}^{m\times 3}$ contain the first three columns of $C_{\delta x}$. By direct integration, disregarding the noise

$$\delta(t) = 2C_{\delta x}x(0) + 2tC_{\delta x}^{1:3}v^n(0) + t^2 C_{\delta x}^{1:3} f^n(0). \tag{21}$$

Due to Assumption 4, $\mathrm{rank}(C_{\delta x}) = 4$ and $x(0) = C_{\delta x}^+\delta(0)/2$ are well defined. Let $T > 0$ be arbitrary and consider two instances of (21) for $t = T/2$ and $t = T$

$$\delta\left(\frac{T}{2}\right) = C_{\delta x}C_{\delta x}^+\delta(0) + TC_{\delta x}^{1:3}v^n(0) + \frac{1}{4}T^2C_{\delta x}^{1:3}f^n(0)$$

$$\delta(T) = C_{\delta x}C_{\delta x}^+\delta(0) + 2TC_{\delta x}^{1:3}v^n(0) + T^2C_{\delta x}^{1:3}f^n(0).$$

It follows that:

$$\begin{pmatrix} TI_3 & \frac{1}{4}T^2I_3 \\ 2TI_3 & T^2I_3 \end{pmatrix}\begin{pmatrix} v^n(0) \\ f^n(0) \end{pmatrix} = \begin{pmatrix} C_{\delta x}^{1:3} & 0 \\ 0 & C_{\delta x}^{1:3} \end{pmatrix}^{-1} \cdot \begin{pmatrix} \delta\left(\frac{T}{2}\right) - C_{\delta x}C_{\delta x}^+\delta(0) \\ \delta(T) - C_{\delta x}C_{\delta x}^+\delta(0) \end{pmatrix}.$$

Assumption 4 gives $\mathrm{rank}(C_{\delta x}^{1:3}) = 3$, and it is straightforward to show that the left matrix is nonsingular for any $T > 0$. Hence, we have a constructive proof that the full state can be computed as a function of the measurements of $\delta(t)$ on any nonzero time interval T. ∎

Remark 3: When $m \leq 4$, the system (A, C) may not be UO. In particular, as shown in the Appendix, the solution to the algebraic measurement equation may not be unique. The observer can also be modified to deal with this situation. When $m \leq 4$ is an intermittent situation that occurs for short periods of time due to loss of measurements, the observer may be operated as it is. If $m = 4$ is the general situation, a GES observer can still be designed by using z as measurement and $\hat{z} = 2C_{zw}\hat{x} + \ell\hat{r}$ as predicted measurement in place of δ and $\hat{\delta}$. Since the variable r cannot be eliminated and there exist in general two ambiguous solution alternatives, we need to estimate $\hat{r}$ using (26) and resolve the ambiguity using domain knowledge.

Remark 4: It is also relatively straightforward to extend the observer using range-rate (Doppler) measurements, employing models similar to the one in [14].

C. Stability and Selection of Gain Matrix

In this section, we first derive conditions for GES of the nominal observer, i.e., when there is no measurement noise. We then propose a Riccati-based method for selection of time-varying gain matrix K and discuss its tuning, given measurement noise variances and the stability requirements resulting from the feedback interconnection of the attitude and translational motion observers.

GES of the feedback interconnection of the two observers was established in [11] using small-gain arguments to ensure that the L_2 gain from u to $\tilde{\chi}$ is sufficiently small. The setup in [11] considers loosely coupled integration, which has the simplifying feature that the translational motion observer error dynamics is linear time invariant (LTI) with an integrator chain structure that achieves an arbitrary small L_2 gain of the transfer matrix from u to $\tilde{\chi}$ by choosing the gain matrix K sufficiently large. Then, the attitude estimation error has sufficiently small influence on the translational motion estimation error. In this brief, a more general L_2-gain condition is used instead of the H_∞-norm. Following [16, p. 209], and setting

$\varepsilon = 0$ and $\epsilon_u = 0$, the LTV system (19) has L_2 gain less than γ_0 for any initial condition $\tilde{\chi}(0)$ if there exist a positive semidefinite function $V(\tilde{\chi})$ and constant $a > 0$ with:

$$\begin{aligned}\dot{V} &= \frac{dV}{d\tilde{\chi}}(\tilde{\chi})((A - KC)\tilde{\chi} + Bu) \\ &\leq a\left(\gamma_0^2 \|u\|_2^2 - \|\tilde{\chi}\|_2^2\right). \end{aligned} \tag{22}$$

Assumption 5: The signals δ, f^b, and $\dot{f}^b$ are bounded.

Proposition 1: Let σ^* be as defined in Lemma 1. Assume that $K_P, k_I > 0$, $\sigma \geq \sigma^*$ and that there is no noise. Then, there exists a $\gamma_0 > 0$ such that if K is chosen such that.

1) The nominal system (19) with $u = 0$ is GES.
2) The L_2 gain of the LTV system (19) is less than γ_0.

Then the origin of the error dynamics of $(\tilde{R}, \tilde{b}, \tilde{\chi})$ is GES.

Proof: The proof is similar to [11] since the term in the Lyapunov function corresponding to the translational motion observer can be replaced by V and we can employ (22). We note that u is bounded due to Assumption 5 and Lemma 1. ∎

In general, since the error dynamics is LTV, we propose to select a time-varying gain matrix K by

$$K := PC^T R^{-1} \tag{23}$$

where P satisfies the Riccati equation

$$\dot{P} = PA + A^T P - PC^T R^{-1} CP + Q \tag{24}$$

with $P(0) = P^T(0) > 0$. Next, we show that this can ensure that condition 1) in Proposition 1 is fulfilled.

Proposition 2: Let $Q, R, K_P, k_I > 0$ and $\sigma \geq \sigma^*$, and assume that there is no noise. Then, there exists a $\gamma_0 > 0$ such that if K and P are chosen according to (23) and (24) and the L_2 gain of the LTV system (19) is less than γ_0, then P is uniformly bounded and the origin of the error dynamics of $(\tilde{R}, \tilde{b}, \tilde{\chi})$ is GES.

Proof: It is straightforward to show that $(A, BQ^{1/2})$ is controllable. Since, in addition, the system (A, C) is UO from Lemma 2 and C is bounded due to Assumption 5, it follows from standard properties of the Riccati equation that P is uniformly bounded [17], [18], and the nominal system:

$$\dot{\chi} = (A - KC)\chi$$

is GES. Hence, condition 1) of Proposition 1 is fulfilled, and the result follows immediately since condition 2) is fulfilled by assumption on the L_2 gain. ∎

The covariance matrix R of the measurements δ can be computed by assuming independent white noise on the pseudo-range. The covariance matrix Q can be tuned knowing of the variance of the accelerometer and rate gyro measurements.

We proceed by discussing how the L_2 gain condition can be fulfilled. Clearly, this is theoretically more involved with the LTV model than the LTI model in [11], since the L_2 gain is more difficult to analyze since C is time-varying and its future value is not known. Since the gain K defined by (23) and (24) is not *a priori* guaranteed to satisfy the L_2-gain condition for arbitrary symmetric Q, $R > 0$, one may have to tune the observer parameters Q and R in order to achieve acceptable stability and performance of their interconnection. The intuition behind the L_2-gain condition is that it ensures that an error in the attitude estimate has a sufficiently small effect on the acceleration estimation. Intuitively, a sufficiently large K leading to sufficiently small L_2 gain be determined by choosing R sufficiently small and Q sufficiently large. This means that it may be necessary to redesign the Q and R matrices to different values than those derived from the sensor noise variances, although this was not necessary for the simulations reported in Section IV. In any case, a final-stage estimation step in order to improve estimation accuracy is subsequently described in Section III-D.

Remark 5: Since the matrix A amounts to a chain of integrators, the gain matrix K can be redesigned using a time-scale tuning parameter as in [7]. This approach would provide a rigorous (albeit rather technical) proof that a K meeting the L_2 gain constraint would always exist. On the other hand, our case studies indicate that the simpler design of K proposed above is sufficient in typical cases.

Remark 6: It is relatively straightforward to extend the observer to an earth-centered earth-fixed coordinate frame instead of NED. The observer and associated analysis will contain some additional terms, while the structure of the observers and the theoretical analysis remains the same.

D. Recovery of Performance With Measurement Noise

Due to introduction of the auxiliary variable r, the quasi-linear measurement model may not give optimal estimates (minimum variance of the relevant states) if there is measurement noise, since information about the nonlinear effect $r = -x^T Mx$ in the data is not explicitly used by the quasi-linear estimators. Similarly, the attitude estimates are over-parameterized (with all nine elements of the rotation matrix estimated independently), which is expected to be sub-optimal (not minimum variance) when there is measurement noise.

An approach to recovery of the performance that could have been achieved with an ideal nonlinear filter was proposed in [14]. It was observed that the estimates from the nonlinear observer can be used to define a linearization point of the Taylor-series expansion of the complete nonlinear model of the combined attitude and translational motion dynamics and measurement systems having output y. Using a first-order linearized approximate time-varying model in a second-stage Kalman–Bucy filter in order to produce a second improved estimate leads to a cascade of the GES nonlinear observer and the GES Kalman–Bucy filter that preserves the key benefits of both the nonlinear observer and the second-stage Kalman–Bucy filter (see Fig. 2). We note that this is not an extended Kalman–Bucy filter (EKF) since the linearization does not depend on the state of the Kalman–Bucy filter, such that there is no feedback connection that could lead to instability.

IV. Case Study

We simulate a small fixed-wing unmanned aerial vehicle (UAV) trajectory in a final approach toward landing. The vehicle simulation is based on a nonlinear 6-DOF

TABLE I
SIMULATION CASES

	Case 1 No initial error	Case 2 Typical initial error	Case 3 Large initial error	Case 4 Large initial error	Case 5 Large initial error
Initial horizontal error	0 m	40 m	250 m	100 m	250 m
Initial vertical error	0 m	30 m	0 m	50 m	50 m
Initial time sync (bias) error	0 m	100 m	0 m	100 m	100 m
Initial attitude error	0 deg	$<$ 2 deg	$<$ 15 deg	$<$ 15 deg	$<$ 15 deg

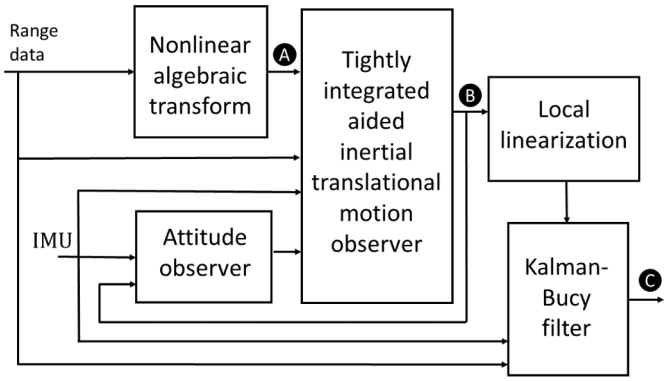

Fig. 2. Final-stage estimation using the linearized Kalman–Bucy filter. Position and velocity estimates are output with increasing accuracy at outputs A–C, respectively.

rigid body dynamic model with aerodynamic parameters corresponding to the Aerosonde UAV [19]. Just before touching the ground it decides to abort the landing, so it climbs out and loiters at a holding position north of the landing target.

In this simulation example, we assume that six radio beacons are distributed within an area with up to 1500-m horizontal separation and with up to 10-m vertical separation between the beacons. The beacons provide signals that are used for pseudorange measurements (e.g., phase or time of arrival) with standard deviation $\sigma_y = 0.25$ m, a constant receiver clock bias corresponding to $\beta = 100$ m, and a sampling interval of 0.1 s. Magnetometer, rate gyro, and accelerometer measurements are available at 0.01 s sampling interval and simulated random noise with standard deviations of 1.15 mG, 0.8°/s, and 0.09 m/s^2, respectively, corresponding to the typical output noise specification of an Analog Devices ADIS 16407 IMU. The gyro has a small constant unknown bias.

Four different estimators are simulated and compared. The first three estimators corresponding to the output of the different stages of the proposed estimator structure (outputs A–C in Fig. 2), while the fourth is a standard EKF, are included for comparison.

1) Algebraic estimator (no filtering) based on the globally valid quasi-linear algebraic model using weighted least squares (see the Appendix).
2) Nonlinear observer discretized using the Euler method and the discrete-time Riccati equation.
3) Nonlinear observer (as above) with second-stage linearized time-varying discrete-time Kalman filter for position, velocity, and range measurement bias.

TABLE II
SIMULATION RESULTS WITH AVERAGED ERRORS DURING THE 125-s FLIGHT PERIOD. BOLD NUMBERS INDICATE LACK OF CONVERGENCE. ITALIC NUMBERS INDICATE BEST PERFORMANCE FOR EACH CASE

	Case 1	Case 2	Case 3	Case 4	Case 5
Avg hor err					
Alg WLS	44.2 m	48.2 m	40.4 m	38.6 m	42.7 m
Nonlin obs	13.9 m	10.9 m	14.1 m	14.1 m	12.1 m
2-stage KF	*2.62 m*	*4.85 m*	*8.96 m*	6.14 m	*6.7 m*
EKF	2.79 m	5.27 m	**141 m**	*6.09 m*	**133 m**
Avg vert err					
Alg WLS	29.3 m	30.2 m	30.7 m	29.8 m	29.5 m
Nonlin obs	4.68 m	5.37 m	7.39 m	8.62 m	7.23 m
2-stage KF	1.10 m	*1.26 m*	*1.89 m*	*1.50 m*	*1.84 m*
EKF	*0.98 m*	1.47 m	**62.1 m**	1.57 m	**59.8 m**

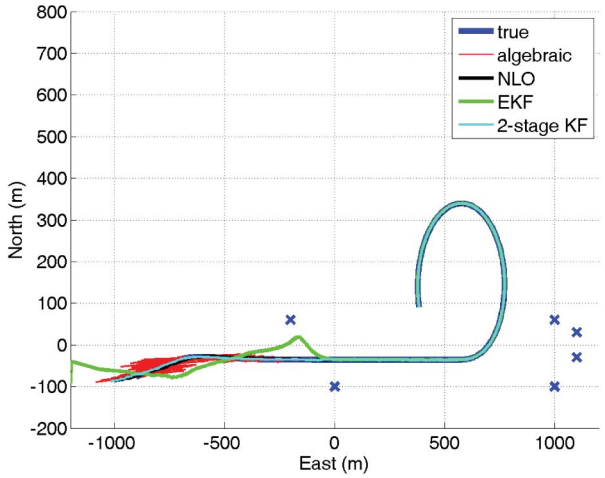

Fig. 3. Horizontal position estimated with different observers. The initial position is at -1100 m east and -80 m north. The six beacon positions are marked by blue crosses.

4) The discrete-time EKF based on a linearization of the model about the current estimate—the EKF is the cascade of a standard discrete-time multiplicative EKF estimating Gibb's vector to update a global quaternion representation of attitude [20], and a standard EKF for the position and velocity estimation, taking the estimated attitude as input.

The nonlinear observer tuning parameters are $K_P = 10I_3$ and $k_I = 10^{-5}$ for the attitude observer. The tuning of all the Kalman filters for translational motion state estimation is based on $Q = \text{diag}(0, 0, 0, 10^{-5}, 10^{-3}, 10^{-3}, 10^{-3}, 10^{-8}, 10^{-8}, 10^{-8})$. The R matrix is computed based on the range measurement standard deviation σ_y. The initial covariance is given by $P(0) = \text{diag}(3 \cdot 10^3, 3 \cdot 10^3, 3 \cdot 10^3, 3 \cdot 10^3, 10, 10, 10, 0.01, 0.01, 0.01)$.

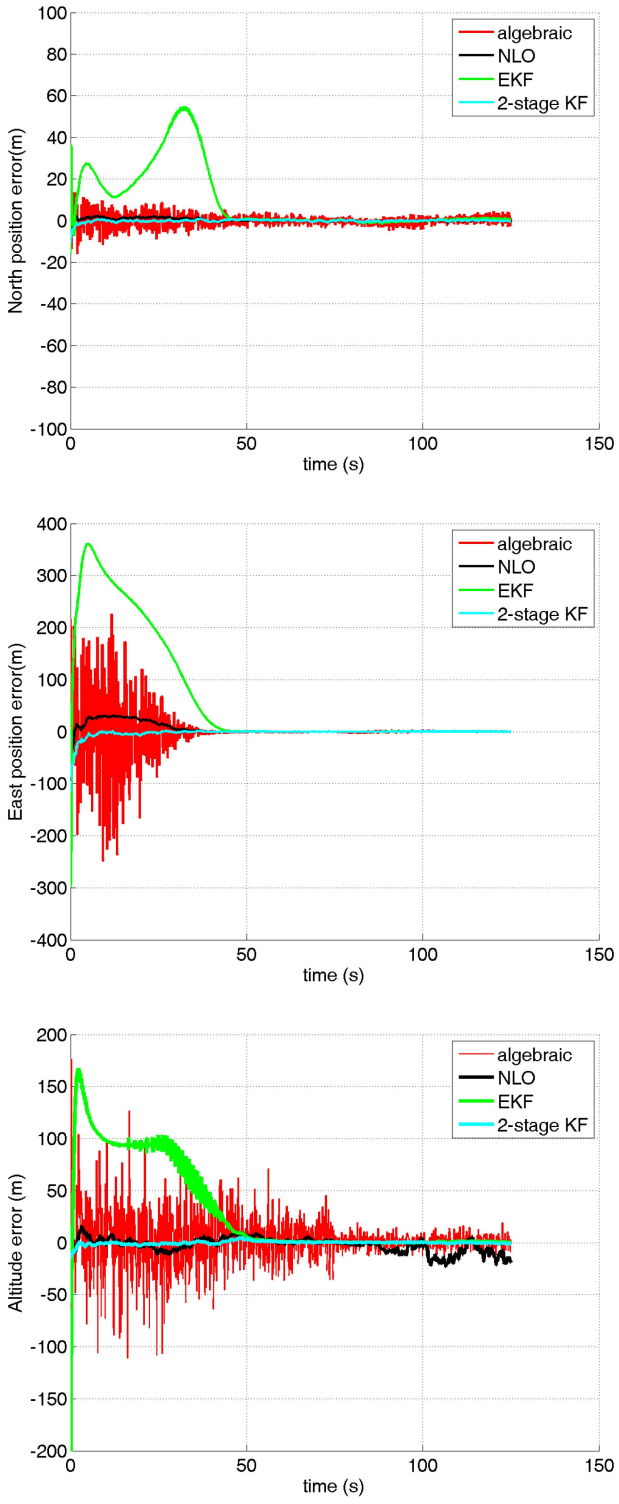

Fig. 4. North, east, and vertical estimation errors.

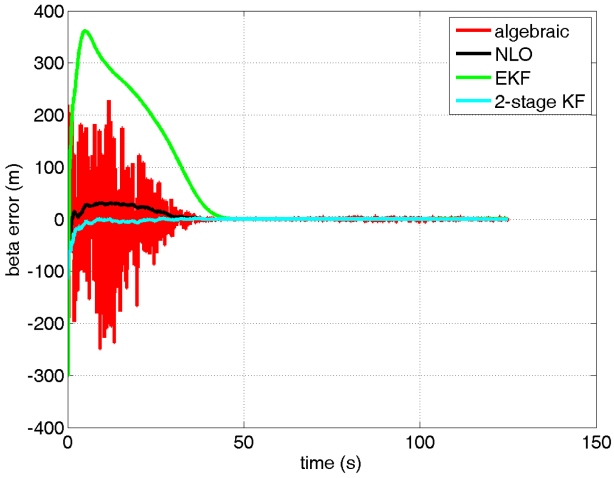

Fig. 5. Range bias β estimated with different observers.

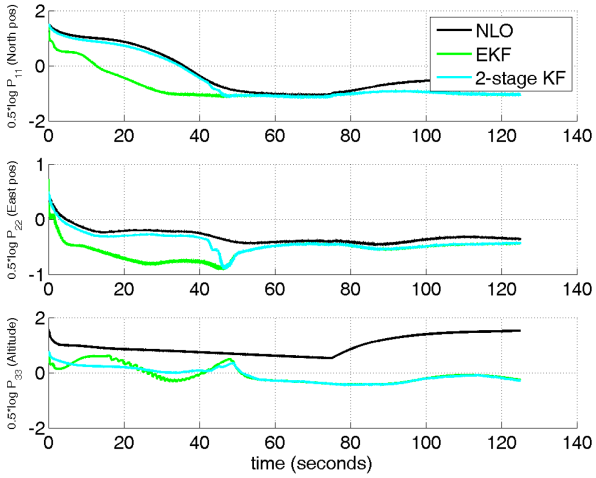

Fig. 6. Square roots of the diagonal elements of covariance matrices corresponding to position estimates. Note the logarithmic scale.

In order to evaluate the performance of the observers, five simulation cases are defined in Table I. The different cases correspond to different initialization errors, ranging from no initial error (Case 1), small initialization error (Case 2), and worst case (but still realistic and typical) initialization errors (Cases 3–5). The simulation results (average estimation errors) are summarized in Table II. The results show that in all cases, the algebraic solution (output A) has the highest error variance, and the nonlinear observer (output B) has a significantly lower error variance, while the second-stage KF (output C) has the lowest error variance among the three. In all cases, the nonlinear observer and the second-stage KF converges without any issues. In comparison, the reference EKF achieves comparable performance as the second-stage KF for Case 1 (no initial error). The EKF's performance degrades to higher error variances than the second-stage KF, in particular in Cases 3 and 5, where the EKF experiences convergence problems leading to large average estimation error. The lack of convergence is caused by too large initialization error in position.

Curves for an extended simulation of Case 5 are given in Figs. 3–6, where the extension is that the number of beacons is reduced from 6 to 4 after time $t = 75$ s. It can be seen that the effect of initial errors in the estimates of position and bias β that are seen to persist for more than 50 s in Figs. 3–5. There is some graceful degradation of performance when switching from 6 to 4 beacons, as expected. The square roots of the

diagonal elements of the covariance matrices corresponding to position estimates from the nonlinear observer, second-stage KF, and the EKF for Case 5 are shown in Fig. 6. It can be seen that these uncertainty estimates are in agreement with the observed error statistics whenever the EKF converges, but when the EKF has initial convergence issues, its covariance estimates strongly underestimates the true covariance indicating that the EKF is trapped in a local minimum.

V. Conclusion

A nonlinear observer approach to tightly coupled integration of INS with pseudorange measurements has been described and found to be GES under some conditions on its tuning parameters.

The simulation example with UAV navigation aided by radio beacons clearly illustrates that the proposed method is able to successfully combine the best features of the nonlinear observer (i.e., global convergence) and the linearized KF (low variance and global convergence) in scenarios where the EKF fails because it depends on accurate initialization.

Appendix

Despite the nonlinear nature of the measurement equation (8), we can exploit their quadratic character to get a relatively simple algebraic solution [1]–[3].

Lemma 3: Let $m \geq 4$ and $\operatorname{rank}(C_{zw}) = 4$. Consider the two candidate solutions given by

$$x = \frac{rc + w}{2}, \quad c = C_{zw}^{+}\ell, \quad w = C_{zw}^{+}z \tag{25}$$

$$r = \frac{-h \pm \sqrt{h^2 - w^T M w \cdot c^T M c}}{c^T M c} \tag{26}$$

where $h := 2 + w^T M c$. If there is no measurement noise and the following condition is satisfied:

$$e = \left(C_{zw}C_{zw}^{+} - I_m\right)(r\ell + z) = 0 \tag{27}$$

then the position solution $p^n = p_0^n + p_\Delta^n$ solves the pseudorange equations (8). Moreover, at least one of the two alternative candidate solutions (25) and (26) is a valid solution that satisfies (27) and is equal to the true position.

For the case $m = 4$, we always have $e = 0$ due to $C_{zw}^{+}C_{zw} = I_4$ since $C_{zw}^{T}C_{zw}$ is nonsingular. Hence, we are guaranteed to have two solutions both satisfying (27), and domain knowledge may be needed to resolve the ambiguity. One example is terrestrial satellite navigation where there is a large distance to the navigation satellites such that nonterrestrial solutions for the vehicle position can be ruled out by checking the vertical position. Another example is underwater navigation, where all transponders are located on the seabed and the vehicle is on the surface or at some distance from the seabed such that positions that are inconsistent with depth measurements can be ruled out. A third example is local navigation for aircraft landing, where transponders are located on the ground and position solutions that are inconsistent with altimeter measurements can be ruled out. A fourth example is the use of bounds on β using knowledge of the measurement system's clock accuracy. This is motivated by the observation that the two alternative solutions typically have significantly different estimated values of β.

For $m \geq 5$, we have only a single solution satisfying (27), except in degenerate cases, where there may be two solutions. Instead of using (25)–(27), this unique solution can be found in a simpler and more direct way by solving the linear system of equations (12).

Lemma 4: Suppose $m \geq 5$ and the matrix $C_{\delta x}$ satisfies $\operatorname{rank}(C_{\delta x}) = 4$. If there is no measurement noise, the unique solution to (12) is given by $x = C_{\delta x}^{+}\delta/2$.

Acknowledgment

The authors would like to thank K. Gryte for providing the UAV flight simulator code used in the example.

References

[1] S. Bancroft, "An algebraic solution of the GPS equations," *IEEE Trans. Aerosp. Electron. Syst.*, vol. 21, no. 1, pp. 56–59, Jan. 1985.

[2] J. Chaffee and J. Abel, "On the exact solutions of pseudorange equations," *IEEE Trans. Aerosp. Electron. Syst.*, vol. 30, no. 4, pp. 1021–1030, Oct. 1994.

[3] D. Dardari, E. Falletti, and M. Luise, Eds., *Satellite and Terrestrial Radio Positioning Techniques*. New York, NY, USA: Academic, 2012.

[4] J. A. Farrell, *Aided Navigation: GPS With High Rate Sensors*. New York, NY, USA: McGraw-Hill, 2008.

[5] P. D. Groves, *Principles of GNSS, Inertial, and Multisensor Integrated Navigation Systems*, 2nd ed. London, U.K.: Artech House, 2013.

[6] R. G. Brown and P. Y. C. Hwang, *Introduction to Random Signals and Applied Kalman Filtering*, 3rd ed. New York, NY, USA: Wiley, 2012.

[7] T. A. Johansen and T. I. Fossen, "Nonlinear observer for inertial navigation aided by pseudo-range and range-rate measurements," in *Proc. Eur. Control Conf.*, Linz, Austria, 2015, pp. 1673–1680.

[8] M. Morgado, P. Batista, P. Oliveira, and C. Silvestre, "Position and velocity USBL/IMU sensor-based navigation filter," in *Proc. 18th IFAC World Congr.*, Milan, Italy, 2011, pp. 13642–13647.

[9] P. Batista, "GES long baseline navigation with unknown sound velocity and discrete-time range measurements," *IEEE Trans. Control Syst. Technol.*, vol. 23, no. 1, pp. 219–230, Jan. 2015.

[10] P. Batista, C. Silvestre, and P. Oliveira, "Sensor-based long baseline navigation: Observability analysis and filter design," *Asian J. Control*, vol. 16, no. 4, pp. 974–994, 2014.

[11] H. F. Grip, T. I. Fossen, T. A. Johansen, and A. Saberi, "Globally exponentially stable attitude and gyro bias estimation with application to GNSS/INS integration," *Automatica*, vol. 51, pp. 158–166, Jan. 2015.

[12] I. Y. Bar-Itzhack and J. Reiner, "Recursive attitude determination from vector observations: Direction cosine matrix identification," *J. Guid., Control, Dyn.*, vol. 7, no. 1, pp. 51–56, 1984.

[13] P. Batista, C. Silvestre, and P. Oliveira, "Sensor-based globally asymptotically stable filters for attitude estimation: Analysis, design, and performance evaluation," *IEEE Trans. Autom. Control*, vol. 57, no. 8, pp. 2095–2100, Aug. 2012.

[14] T. A. Johansen, T. I. Fossen, and G. C. Goodwin, "Three-stage filter for position estimation using pseudo-range measurements," *IEEE Trans. Aerosp. Electron. Syst.*, in press.

[15] H. F. Grip, T. I. Fossen, T. A. Johansen, and A. Saberi, "Attitude estimation using biased gyro and vector measurements with time-varying reference vectors," *IEEE Trans. Autom. Control*, vol. 57, no. 5, pp. 1332–1338, May 2012.

[16] H. K. Khalil, *Nonlinear Systems*. Englewood Cliffs, NJ, USA: Prentice-Hall, 2002.

[17] R. E. Kalman and R. S. Bucy, "New results in linear filtering and prediction theory," *J. Basic Eng.*, vol. 83, no. 1, pp. 95–109, 1961.

[18] B. D. O. Anderson, "Stability properties of Kalman–Bucy filters," *J. Franklin Inst.*, vol. 291, no. 2, pp. 137–144, 1971.

[19] R. W. Beard and T. W. McLain, *Small Unmanned Aircraft: Theory and Practice*. Princeton, NJ, USA: Princeton Univ. Press, 2012.

[20] F. L. Markley, "Attitude error representations for Kalman filtering," *J. Guid., Control, Dyn.*, vol. 26, no. 2, pp. 311–317, 2003.